OMICS A Journal of Integrative Biology
Volume 17, Number 1, 2013

DOI: 10.1089/omi.2011.0035

Original Articles

Metabolomics Reveals Differential Levels of Oral Metabolites in HIV-Infected Patients: Toward Novel Diagnostic Targets

Mahmoud A. Ghannoum,[1] Pranab K. Mukherjee,[1] Richard J. Jurevic,[2] Mauricio Retuerto,[1] Robert E. Brown,[3] Masoumeh Sikaroodi,[3] Jennifer Webster-Cyriaque,[4] and Patrick M. Gillevet[3]

Abstract

The objective of the current study was to characterize the profile of oral metabolites in HIV-infected patients using metabolomics. Oral wash samples were collected from 12 HIV-infected and 12 healthy individuals (matched for age, sex, and ethnicity), processed, and analyzed by metabolomics. We detected 198 identifiable and 85 nonidentifiable metabolites; 27 identifiable metabolites were differentially present (12 increased, 15 decreased) in HIV-infected patients. Elevated metabolites included *p*-cresol sulfate, nucleotides (e.g., allantoin), and amino acids (e.g., phenylalanine, tryptophan), whereas decreased oral metabolites included fucose, fumarate, and N-acetylglucosamine. Pathway network analysis revealed the largest multinode network in healthy versus HIV-infected patients to involve carbohydrate biosynthesis and degradation. HIV-infected patients on antiretroviral therapy (ART) showed the largest number (12) of statistically significant metabolite correlation differences compared with healthy controls. Interestingly, the oral phenlyalanine:tyrosine ratio increased in ART-naive HIV-infected patients (mean $\pm$ SEM $= 2.58 \pm 0.87$) compared with healthy individuals (1.33 ± 0.10, $p = 0.062$) or ART-experienced patients (1.78 ± 0.30, $p = 0.441$). This is the first study to reveal differential levels of oral metabolites in HIV-infected patients compared withj healthy volunteers, and that oral phenlyalanine:tyrosine ratio may be a useful marker for noninvasive monitoring of the immune status during HIV infection.

Introduction

The oral cavity plays an important role in providing insight into the status/progression of HIV disease as the occurrence of specific lesions, mainly oral candidiasis and hairy leukoplakia (Patton et al., 2002; Shiboski et al., 2009). With recent advances in high-throughput technologies, it has been suggested that "-omics" disciplines, such as metabolomics and proteomics, should be applied to reach a deeper understanding of the molecular mechanisms underlying oral disorders (Garcia and Tabak, 2008). Metabolites (small molecules including amino acids, sugars and lipids) present in the oral cavity are produced by both the host and microbes, and are likely to contribute to health and disease (Pendyala et al., 2007; Sreekumar et al., 2009; Sugimoto et al., 2010). Similar to the oral lesions, oral metabolites may also have utility in informing about disease status and/or treatment compliance by acting as diagnostic markers. Thus, profiling the oral metabolites is a prerequisite to defining the mechanisms underlying oral diseases in HIV-infected patients and the discovery of diagnostic targets.

Metabolomics is increasingly being used to accurately measure the spectrum of biochemical changes and map them to metabolic pathways, and has utility in the discovery of disease biomarkers and drug targets. For example, metabolomics has been used to characterize the metabolites present in cancer patients (Denkert et al., 2006, 2008; Sreekumar et al., 2009; Yan et al., 2008), and several studies have suggested associations between different metabolites and cancer Recent studies have also investigated the link between metabolites and oral cancer, where investigators used this approach to identify profiles specific to oral, breast, pancreatic, and oral squamous cell carcinoma (Sugimoto et al., 2010; Zhou et al., 2009).

The progresses in oral pathologies using purely genomic approaches have been overall limited (Diehl, 2006). To date, no study has been performed to characterize oral metabolites in the background of HIV infection, and to determine whether specific metabolites correlate with HIV disease progression and response to antiretroviral therapy (ART). In the current study, to gain insight into oral metabolites and their association with HIV disease, we used metabolomics to compare the oral metabolome in healthy subjects and participants with

[1]Center for Medical Mycology, Case Western Reserve University, and University Hospitals Case Medical Center, Cleveland, Ohio.
[2]Case Western Reserve University, School of Dentistry, Cleveland, Ohio.
[3]George Mason University, Manassas, Virginia.
[4]University of North Carolina, Chapel Hill, North Carolina.

HIV infection. Analysis of oral wash samples showed differential levels of metabolites in HIV-infected patients compared with healthy subjects, including those involved in amino acid and carbohydrate metabolic pathways.

Materials and Methods

Ethical conduct of research statement

Written informed consent was obtained from all participants in this study. Recruitment of study participants was performed according to protocol (#20070413) approved by the Human Subjects Institution Review Board (IRB) of Case Western Reserve University, Cleveland (OH), and UH/Case Medical Center CFAR, Cleveland (OH).

Study participants

Oral rinse samples were collected from 12 healthy individuals and 12 HIV-positive patients, age, gender, and self-reported ethnicity matched. Informed consent was obtained following review of the IRB at Case Western Reserve University/University Hospitals Case Medical Center. The subjects were all from the Cleveland Ohio area and on standard Western diets. The healthy controls were recruited from students and staff at the School of Dental Medicine, or School of Medicine at Case Western Reserve University (CWRU). HIV-positive subjects were recruited from the University Hospitals Case Medical Center, Center for AIDS Research unit (CFAR) and were patients of record in the CFAR unit.

Summary of demographic information of subjects enrolled in the study is provided in Table 1. Self-reported ethnicities of the study participants were classified based upon U.S. Census criteria for classification of race (http://www.census.gov). Race has been classified as White (including Hispanic, East Indian, or European), Black/African American, Asian, and Native American/Native Alaskan, etc. Current antiretroviral medications, most recent viral load and CD4 counts and smoking status, in addition to age, gender, and ethnicity were collected from HIV-infected participants.

Inclusion criteria were age greater than 18 years, and no clinical signs of oral mucosal disease. Exclusion criteria were recent use of antimicrobial or antifungal agents, use of topical or systemic steroids, pregnancy, and insulin-dependent diabetes mellitus.

Sample collection

Concentrated oral rinse has been previously used for the detection of the presence of oral bacteria and fungi (Sedgley and Samaranayake, 1994; White et al., 2004; Yan et al., 2008). Oral rinse (10 mL 0.9% sterile saline) was utilized for this study because (1) it's simple and noninvasive to collect; (2) it's safe to handle compared to other body fluids (blood); (3) its oral cavity is a primary entry point for microbes into the body; (4) oral rinse provides a better representation of the oral chamber environment, and enables the collection of organisms from the dorsum of the tongue, floor of the mouth, palate, posterior pharynx, and buccal mucosal environment; (5) it

Table 1. Summary of Participants' Demographics

ID	*Health status*	*ART status*	*Age*	*Gender*	*Ethnicity*	*CD4 count (cells/mL)*	*Viral load (copies/mL)*	*Medication*
Healthy Controls								
1C	Healthy	—	34	M	H (W)	NA	NA	None
2C	Healthy	—	46	M	C (W)	NA	NA	None
3C	Healthy	—	59	M	AA	NA	NA	None
4C	Healthy	—	22	M	C (W)	NA	NA	None
5C	Healthy	—	37	M	AA	NA	NA	None
6C	Healthy	—	34	F	H (W)	NA	NA	None
7C	Healthy	—	40	M	C (W)	NA	NA	None
8C	Healthy	—	27	M	C (W)	NA	NA	None
9C	Healthy	—	53	M	AA	NA	NA	None
10C	Healthy	—	44	M	AA	NA	NA	None
11C	Healthy	—	22	M	AA	NA	NA	None
12C	Healthy	—	47	M	AA	NA	NA	None
ART-experienced HIV-infected patients								
2	HIV-infected	ART-experienced	56	M	AA	639	75	Atripla
3	HIV-infected	ART-experienced	52	M	AA	800	48	Atripla
4	HIV-infected	ART-experienced	40	M	C (W)	947	48	Atripla
5	HIV-infected	ART-experienced	40	M	C (W)	280	48	Atripla
7	HIV-infected	ART-experienced	31	F	H (W)	1,029	48	Ritonavir, Fosamprenavir, Combivir
8	HIV-infected	ART-experienced	42	M	AA	814	53	Ritonavir, Atazanavir, Truvada
11	HIV-infected	ART-experienced	31	M	C (W)	670	68	Atripla
12	HIV-infected	ART-experienced	45	M	AA	899	48	Ritonavir, Atazanavir, Truvada
ART-naive HIV-infected patients								
1	HIV-infected	ART-naive	31	M	H (W)	380	158,000	None
6	HIV-infected	ART-naive	22	M	AA	966	1,100	None
9	HIV-infected	ART-naive	22	M	C (W)	581	115,000	None
10	HIV-infected	ART-naive	52	M	AA	5	185,000	None

ART, antiretroviral therapy; W, White; H, Hispanic; C, Caucasian; AA, African-American.

facilitates collection of oral chamber metabolites. Oral samples were collected at least 1 h after a meal, at approximately the same time for all participants (9–11 a.m.). This was done to limit contamination of samples with extraneous components and standardize the possible impact of variation in salivary flow rates. Study participants were provided a 10-mL syringe with 0.9% sterile normal saline. The subjects were instructed to inject the contents into their mouth and swish for 1 min, after which time were to expectorate into a sterile 50-mL conical tube. Samples were then stored on ice until it was transported back to the lab for processing (within 2 h). The collected samples were then centrifuged at $3{,}500 \times g$ for 20 min at 4°C to separate the cells (pellet) from the extra cellular soluble components (supernatant). The supernatant extracted with acetonitrile and processed for metabolome analysis (as described below). Each sample received was accessioned into the Laboratory Information Management System (LIMS) at Metabolon and was assigned a unique identifier, and bar coded. The unique identifier and bar codes were used to track all samples (and all derived aliquots), tasks, and results. All samples were maintained at −80°C until processed.

Sample processing

The sample preparation process was carried out using the automated MicroLab STAR® system (Hamilton Company, Reno, NV), as described earlier (Cantor, 2010; Dehaven et al., 2010; Evans et al., 2009; Ohta et al., 2009; Takei et al., 2010). Recovery standards were added prior to the first step in the extraction process for quality control (QC) purposes. Sample preparation was conducted using a series of organic and aqueous extractions to remove the protein fraction while allowing maximum recovery of small molecules. The resulting extract was divided into two fractions: one for analysis by liquid chromatography (LC) and the second for analysis by gas chromatography (GC). Samples were placed briefly on a TurboVap® (Zymark) to remove the residual organic solvent. Each sample was then frozen and dried under vacuum, and prepared for LC/mass spectrometry (MS) or GC/MS. A small aliquot of each experimental sample for a specific matrix was obtained and pooled together as a "Client matrix" (CMTRX). Aliquots of these CMTRX samples were injected throughout the platform day run and serve as technical replicates. Such analysis allows monitoring of variability in the quantitation of the detected biochemicals in the experimental samples. With this monitoring, a metric for overall process variability can be assigned for the platform's performance based on the quantitation of metabolites in the actual experimental samples.

LC/MS, LC/MS2

The LC/MS portion of the platform is based on a Waters Acquity UPLC and a Thermo-Finnigan LTQ mass spectrometer, which consists of an electrospray ionization (ESI) source and linear ion-trap (LIT) mass analyzer. The sample extract was split into two aliquots, dried, then reconstituted in acidic or basic LC-compatible solvents, each of which contain 11 or more injection standards at fixed concentrations. One aliquot was analyzed using acidic positive ion optimized conditions and the other using basic negative ion optimized conditions in two independent injections using separate dedicated columns. Extracts reconstituted in acidic conditions were gradient eluted using water and methanol both containing 0.1% formic acid, while the basic extracts, which also used water/methanol, contained 6.5 mM ammonium bicarbonate. The MS analysis alternates between MS and data-dependent MS2 scans using dynamic exclusion.

Accurate mass determination and MS/MS fragmentation (LC/MS), (LC/MS/MS)

The LC/MS accurate mass portion of the platform was based on a Waters Acquity UPLC and a Thermo-Finnigan LTQ-FT mass spectrometer, which has a linear ion-trap (LIT) front end and a Fourier transform ion cyclotron resonance (FT-ICR) mass spectrometer backend. For ions with counts greater than 2 million, an accurate mass measurement can be performed. Accurate mass measurements can be made on the parent ion as well as fragments. The typical mass error is less than 5 ppm. Ions with less than 2 million counts require a greater amount of effort to characterize. Fragmentation spectra (MS/MS) are typically generated in data-dependent manner, but if necessary, targeted MS/MS can be employed, such as in the case of lower level signals.

GC/MS

The samples destined for GC/MS analysis were redried under vacuum desiccation for a minimum of 24 h prior to being derivatized under dried nitrogen using bistrimethylsilyl-triflouroacetamide (BSTFA). The GC column used was 5% phenyl and the temperature ramp was from 40° to 300°C in a 16-min period. Samples were analyzed on a Thermo-Finnigan Trace DSQ fast-scanning single-quadrupole mass spectrometer using electron impact ionization. The instrument was tuned and calibrated for mass resolution and mass accuracy on a daily basis. The information output from the raw data files were automatically extracted as discussed below.

Bioinformatics

The informatics system consisted of four major components, the Laboratory Information Management System (LIMS), the data extraction and peak-identification software, data processing tools for QC and compound identification, and a collection of information interpretation and visualization tools for use by data analysts. The hardware and software foundations for these informatics components were the LAN backbone, and a database server running Oracle 10.2.0.1 Enterprise Edition.

Compound identification

Biochemicals were identified by comparison to library entries of purified standards or recurrent unknown entities. Identification of known chemical entities was based on comparison to metabolomic library entries of purified standards. Approximately 1,500 commercially available purified standard biochemicals have been acquired and registered into LIMS for distribution to both the LC and GC platforms, for determination of their analytical characteristics. The combination of chromatographic properties and mass spectra give an indication of a match to the specific compound or an isobaric entity. Additional chemical entities can be identified by virtue of their recurrent nature (both chromatographic and mass spectral). These biochemicals have the potential to be

identified by future acquisition of a matching purified standard or by classical structural analysis.

Curation

A variety of curation procedures were carried out to ensure that a high-quality data set was made available for statistical analysis and data interpretation. The QC and curation processes were designed to ensure accurate and consistent identification of true chemical entities, and to remove those representing system artifacts, mis-assignments, and background noise. Library matches for each compound were checked for each sample and corrected if necessary.

Normalization

For studies spanning multiple days, a data normalization step was performed to correct variation resulting from instrument interday tuning differences. Essentially, each compound was corrected in run-day blocks by registering the medians to equal one (1.00) and normalizing each data point proportionately (termed the "block correction"). For studies that do not require more than 1 day of analysis, no normalization was necessary, other than for purposes of data visualization.

Differential correlation network (DCN)

Performing DCN analysis allows sifting through large volumes of data and focuses on potentially significant relationships between metabolites and enhances the ability to interpret a complex oral environment (Giacomelli and Covani, 2010). This technique supports knowledge discovery and hypotheses generation by extracting significantly different correlations between same metabolite pairs in class 1 versus class 2. The data generated in our study were comprised of three classes (metabolome variants): (1) healthy controls, (2) HIV-infected (ART-naive and -experienced), and (3) ART-experienced HIV-infected patients. One hundred ninety-eight known metabolites were measured for each sample in each class. First, each class was analyzed internally for significant metabolite pair correlations using the Spearman Rank correlation (we chose Spearman correlation for this analysis to address issues with small sample sizes, and the inability to assume parametric data). Next, metabolite pair correlations within each class were assessed to determine if there is a significant difference in the pair's correlation across classes. The significance of the correlation differential was determined using the z-value statistic (Morgenthal et al., 2006), then converted to a significance probability. Because there were only 12 patients in each group, significant differences were concluded based on the relaxed statistical cutoff of $p < 0.2$ (using Wilcoxon Rank Sum Test) (Sreekumar et al., 2009). All metabolite data were included in the correlation analysis. Determination of a metabolite pair correlation required three samples in the same class, with measureable values for both of the sample metabolites. The metabolites (nodes) were color coded by their KEGG superpathway; edges reflecting differential correlations between metabolite nodes are either red, if the correlation differential network for the healthy versus the HIV experienced classes, or green, for the DCN for the healthy versus the All-HIV class. The edge labels indicate the significance probability associated with the correlation differential determined above.

Results

Oral metabolites are differentially produced in HIV infection

A prerequisite to understanding the effect of oral metabolites on initiation and progression of HIV disease is to define their profile in HIV-infected patients compared with healthy individuals. Therefore, we compared the metabolite profile of oral wash samples obtained from 12 HIV-infected and 12 healthy individuals matched for gender (92% males, 8% females), ethnicity (Hispanic, 17%; African-American, 50%; Caucasian, 33%), and age (mean age 39 years) (see Table 1 for participant demographics). The metabolomic data generated for the two groups (healthy and HIV-infected) were compared by the nonparametric Wilcoxon Rank Sum Test, following log transformation and imputation with minimum observed values for each compound. Our results showed the presence of 198 identifiable and 85 nonidentifiable metabolites. Among the identifiable metabolites, 27 were differentially present (12 increased, mainly amino acids; 15 decreased, mainly carbohydrates) in HIV-infected patients (Table 2, and supporting Supplementary Table ST1). Metabolites with elevated levels included *p*-cresol sulfate, nucleotides (e.g., allantoin, thymine, AMP), amino acids (e.g., Trp, Phe, Tyr) and the tyrosine-derivative tyramine. Metabolites with decreased levels in HIV-infected patients included fucose, fumarate, and N-acetylglucosamine. Some of the differentially present metabolites (e.g., *p*-cresol sulfate, tyramine, allantoin) are known to be associated with microbial activity.

DCN analysis revealed differences in metabolic pathways between healthy individuals and HIV-infected patients

To obtain a biological process perspective of the metabolites in the oral cavity of healthy and HIV-infected patients, we performed DCN analysis on the data using Python-based Spearman correlation algorithm, and the resulting networks were visualized with the open source Cytoscape Network visualization package (www.cytoscape.org) (Cline et al., 2007; Shannon et al., 2003), with the Metscape plug-in (Gao et al., 2010). Our analyses revealed interconnected nodes spanning across several metabolic superpathways, with some metabolites (e.g., taurine) presenting a large number of connections to other metabolites (Fig. 1; see supporting Supplementary Figs. SF1 and SF2 and supporting Supplementary Table ST2 for list of KEGG IDs used to generate the network pathways). Several smaller sets of interconnected nodes were also detected, demonstrating increased or decreased metabolism in the amino acid and nucleotide superpathways.

Correlation differences were calculated for two groups: (1) healthy versus ART–experienced HIV-infected patients (red edges, Fig. 2A), and (2) healthy versus HIV-infected (including ART-naive and -experienced) patients (green edges, Fig. 2B). Our results showed that the largest cluster of statistically significant metabolite correlation differences detected for Group A involves six metabolites (indicating significantly differentiated metabolism in ART-experienced patients compared with healthy individuals), of which five metabolites were those involved in amino acid and nucleotide superpathways (Fig. 2A). In contrast, for Group B, the largest multinode cluster of the DCN involved differential

Table 2. Heat Map Display of Differentially Expressed Identifiable Metabolites in HIV-Infected and Healthy Individuals

Superpathway	*Pathway*	*Metabolite*	*Fold change (HIV/healthy)*	p-*Value*
Amino acid	Alanine and aspartate metabolism	N-Acetylaspartate (NAA)	0.32	0.01
	Glutamate metabolism	Gamma-aminobutyrate (GABA)	0.38	0.17
	Glycine, serine, and threonine metabolism	Betaine	1.36	0.13
	Lysine metabolism	Cadaverine	1.67	0.16
	Phenylalanine and tyrosine metabolism	*p*-Cresol sulfate	4.46	0.03
	Phenylalanine and tyrosine metabolism	Phenylalanine	1.39	0.09
	Phenylalanine and tyrosine metabolism	Tyramine	4.17	0.06
	Tryptophan metabolism	Indolelactate	2.01	0.16
	Tryptophan metabolism	Tryptophan	1.95	0.18
	Urea cycle; arginine-, proline-, metabolism	Arginine	0.65	0.14
	Valine, leucine, and isoleucine metabolism	Isoleucine	2.45	0.14
Carbohydrate	Aminosugars metabolism	Fucose	0.45	0.09
	Aminosugars metabolism	N-Acetylglucosamine	0.33	0.09
	Aminosugars metabolism	N-Acetylneuraminate	0.42	0.11
	Fructose, mannose, galactose, starch, and sucrose metabolism	Galactose	0.34	0.02
	Fructose, mannose, galactose, starch, and sucrose metabolism	Sucrose	0.06	0.14
	Glycolysis, gluconeogenesis, pyruvate metabolism	Pyruvate	0.39	0.12
	Nucleotide sugars, pentose metabolism	Xylose	0.37	0.08
Energy	Krebs cycle	Fumarate	0.72	0.18
Lipid	Carnitine metabolism	Succinylcarnitine	0.7	0.07
	Inositol metabolism	*scyllo*-inositol	0.42	0.04
Nucleotide	Purine metabolism, adenine containing	Adenosine 5′-monophosphate (AMP)	3.89	0.10
	Purine metabolism, urate metabolism	Allantoin	4.32	0.06
	Pyrimidine metabolism, thymine containing	Thymine	1.82	0.01
Peptide	Dipeptide	Glycyltyrosine	0.71	0.16
	Dipeptide	Leucylisoleucine	3.89	0.20
Xenobiotics	Benzoate metabolism	Hippurate	0.73	0.07

Red and green cells indicate a significant increase and decrease, respectively, in the levels of metabolites in HIV group relative to healthy controls. Overall fold change was calculated using samples from all HIV-infected patients. Our results showed that levels of amino acids and nucleic acid catabolites were generally elevated, while that of carbohydrates were generally reduced, suggesting active catabolic or fermentative processes.

correlations between seven metabolites based on the KEGG superpathways; for xenobiotics, plus cofactors and vitamins. Other smaller sets of interconnected nodes were also observed, where increased and decreased metabolism in the amino acid and nucleotide superpathways were noted. Overall, 42 significant interactions between metabolite pairs were observed in Group A (healthy versus ART-experienced HIV-infected patients), whereas 18 interactions were detected for metabolite pairs in Group B (healthy versus all HIV-infected patients) (Fig. 2C). Interestingly, four interactions were common to both groups, albeit with differing significance probabilities; these four metabolite pairs were: valerate–4-hydroxyphenylpyruvate, 4-hydroxyphenylpyruvate–isocaproate, isocaproate–caproate, and 1-kestose–sucrose.

These results showed specific changes in metabolic profile between healthy and HIV-infected patients.

Association between metabolite levels and ART status

We found significant increase in the levels of 17 metabolites in ART-naive patients compared to ART-experienced patients (Table 3, $p < 0.05$). These elevated metabolites included aspartate, phenylacetate, indole acetate, and sarcosine. Interestingly, levels of tyramine exhibited a reverse pattern, being decreased in ART-naive patients compared with ART-experienced HV-infected patients. In addition, among HIV-infected patients, levels of 23 metabolites were positively correlated with viral load with a correlation coefficient (Spearman's rho) ranging between 0.747 for ethanolamine ($p = 0.005$) and 0.548 for N-acetylaspartate (NAA, $p = 0.065$). In contrast, tyramine levels were negatively correlated with viral load (Spearman's rho $= -0.645$, $p = 0.023$).

Differential levels of phenylalanine and tyrosine are associated with HIV disease and ART

Blood phenylalanine-to-tyrosine ratio has been shown to increase in HIV-1 infected pateints, which decreased following ART (Zangerle et al., 2010). Therefore, in the current study, we investigated whether similar patterns also exist in oral washes of ART-naive and ART-experienced HIV-infected patients. We found that levels of tryptophan and phenylalanine tended to increase in ART-naive patients, whereas tyrosine levels remained unchanged between ART-naive and

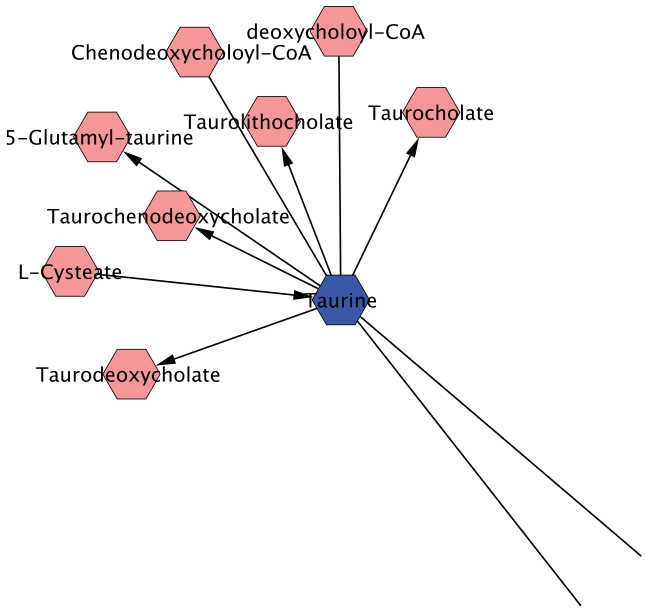

FIG. 1. Network connections with a representative metabolite (taurine) present differentially in healthy and HIV-infected patients, interconnected with other metabolites or pathways. Data were analyzed using the Metscape plugin in the open-source Cytoscape software. (Enlarged version of this figure showing all identified metabolites can be viewed in Supplemental Fig. SF1. Data used to generate the Cytoscape network visualization has been provided as Supplemental Table ST2.)

ART-experienced HIV-infected patients (Fig. 3). Fucose levels also remained similar among the healthy and HIV-infected patient groups. Furthermore, the oral Phe:Tyr ratio increased in ART-naive HIV-infected patients (mean $\pm$ SEM $= 2.58 \pm 0.87$) compared with healthy (1.33 ± 0.10, $p = 0.062$) individuals or ART-experienced patients (1.78 ± 0.30, $p = 0.441$). The oral Phe:Tyr ratio of ART-experienced patients were similar to that of healthy individuals ($p = 0.792$).

Discussion

In the current study, we identified the metabolites present in the oral cavity of HIV-infected patients, and compared this metabolomic profile to that of healthy individuals. We also determined whether changes in the metabolomic profile are associated with HIV disease and response to ART.

Our results showed differential production of specific metabolites in response to HIV infection. These metabolites included those that are common to host and microbes, or known to be of microbial origin (e.g., *p*-cresol sulfate, allantoin). Samples obtained from HIV-infected patients exhibited evidence of heightened activity for several catabolic processes relative to the healthy controls, especially for those related to amino acid metabolism. In this regard, levels of tyramine and *p*-cresol sulfate (both catabolites of tyrosine), were elevated. Tyramine is a monoamine decarboxylation product of tyrosine that can be formed by fermentation processes (Suzzi and Gardini, 2003). Metabolism of tyrosine and phenylalanine by the intestinal flora is known to result in the formation of *p*-cresol (Curtius et al., 1976), which is further converted by cytosolic sulphotransferase into *p*-cresol–sulfate (Burchell and Coughtrie, 1997). *p*-Cresol sulfate is a common component of blood plasma and urine and is considered a uremia toxin in the treatment of kidney disease because it is not efficiently removed by dialysis. This metabolite exhibits a pro-inflammatory effect on unstimulated leucocytes and may contribute to development of vascular disease in uremic population (Schepers et al., 2007). The presence of *p*-cresol sulfate in oral washes of HIV-infected patients suggests that these patients may have underlying kidney disease. In this regard, the prevalence of chronic kidney disease (CKD) in HIV-infected patients ranges globally between 1.1% and 48.5% (Naicker and Fabian, 2010; Volberding and Deeks, 2010). Consequently, early detection programs to assist in detecting and managing CKD have been proposed as a way to provide clinical and cost-effective management of CKD (Katz et al., 2010). Studies investigating the correlation between oral *p*-cresol sulfate and kidney function in HIV-infected patients are warranted.

Elevated levels were also observed for cadaverine and indolelactate, which are breakdown products of lysine and tryptophan, repspectively. Cadaverine is a bacterial product that has been associated with oral pathologies including periodontal disease and bad breath (Barnes et al., 2009; Levine et al., 2001; Rosenberg, 2002; Scully et al., 1997; Walters, 1987). Recently, Shah et al. (2010) showed that cadaverine biosynthesis is crucial for fitness and pathogenesis of *Streptococcus pneumoniae*, a common oral pathogen. These investigators showed that mutants deficient in polyamine biosynthesis (*ΔspeE* or *Δcad*) or transport genes (Δ*potABCD*) were attenuated in murine models of pneumococcal colonization and pneumonia either alone or in competition with wild-type strain. Given these findings, it is possible that elevation of cadaverine levels in HIV-infected patients in our study may impact the diversity of the oral microbiome in this patient population relative to healthy controls. Elevated levels of indolelactate may suggest defects in tryptophan metabolism.

Network analyses revealed the presence of several metabolites representing amino acid biosynthesis and carbohydrate metabolism pathways. Some of these metabolites (e.g., glycine, sorbitol) are involved in overlapping metabolic processes, and may represent key regulatory points of the overall metabolome. These metabolites may also play important roles in regulating host–microbe interactions. Detailed studies investigating these processes are warranted.

Our data showed that levels of some amino acids, for example, phenylalanine and tryptophan, were consistently elevated in the HIV-infected individuals, whereas others like tyrosine remained unchanged in the setting of HIV. The increase in levels of phenylalanine may be due to a reduced activity of the enzyme phenylalanine hydroxylase, which catalyzes the conversion of Phe to Tyr, and is a rate-limiting step in the biosynthesis of dopamine. We also found significant increase in the levels of sarcosine and other metabolites in ART-naive patients compared with ART-experienced patients. Interestingly, Sreekumar et al. (2009) recently identified sarcosine as a potentially mediator of progression of prostate cancer. The role of these metabolites in HIV disease progression needs to be investigated.

Alteration in the levels of amino acids during HIV infection may impact associated opportunists. For example, oral metabolites (e.g., tryptophan) that affect *Candida* growth are likely to impact oral candidiasis, which is among the most

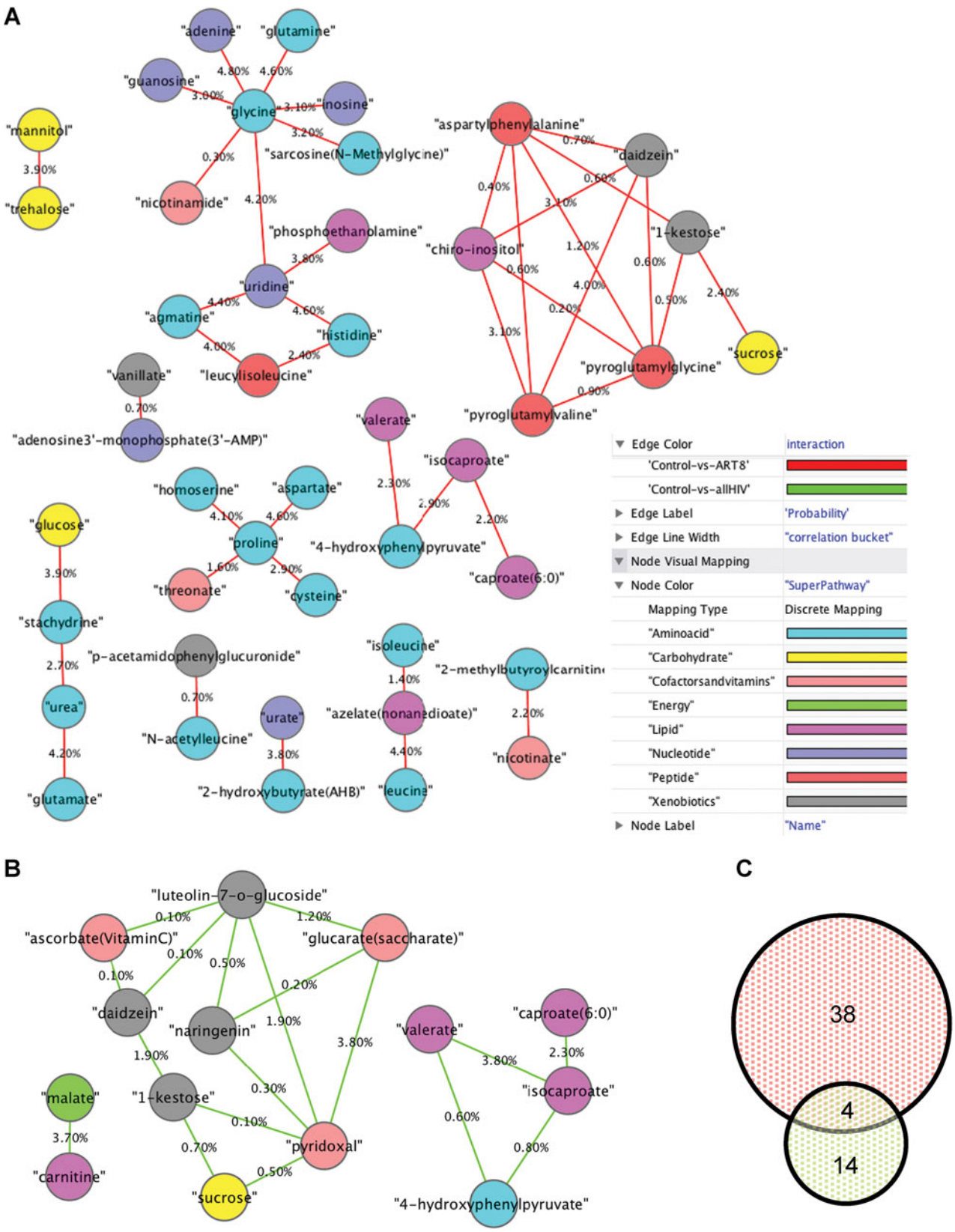

FIG. 2. Differential Correlation Network (DCN) analysis of significant correlations between paired metabolite differences in oral wash samples. Correlation differences were calculated for (**A**) healthy vwersus ART-experienced HIV-infected patients (red edges), and (**B**) healthy versus HIV-infected (including ART-naive and -experienced) patients (green edges). Metabolite differential correlation (edge) is displayed as percentage significant difference. Visualization was created with Cytoscape (www.cytoscape.org), and the metabolites (nodes) were color coded by their KEGG superpathway. (**C**) Depicts the number of interactions between metabolites in sampled obtained from healthy versus ART-experienced HIV-infected patients (red) or healthy versus HIV-infected (green).

Table 3. List of Metabolites with Significant Differences in Levels (Relative Abundance, Mean $\log_{10} \pm$ SD) between ART-Naive and ART-Experienced Patients

Metabolite	*ART-naïve (Mean ± SD)*	*ART-experienced (Mean ± SD)*	p-*Value*[a]
Aspartate	6.66 ± 0.27	6.17 ± 0.23	0.007
N-acetylaspartate (NAA)	4.80 ± 0.10	4.53 ± 0.14	0.006
Serine	6.51 ± 0.32	6.11 ± 0.22	0.029
Glutarate (pentanedioate)	4.65 ± 0.29	4.06 ± 0.45	0.042
3-Phenylpropionate (hydrocinnamate)	5.81 ± 0.42	4.42 ± 0.64	0.003
Phenylacetate	5.44 ± 0.22	4.65 ± 0.42	0.006
Phenyllactate (PLA)	4.82 ± 0.34	4.38 ± 0.21	0.017
Tyramine	4.59 ± 0.31	5.60 ± 0.57	0.008
Putrescine	7.57 ± 0.32	7.20 ± 0.17	0.022
Indoleacetate	5.61 ± 0.52	4.91 ± 0.45	0.036
5-Aminovalerate	7.11 ± 0.30	6.81 ± 0.13	0.034
Sarcosine (N-Methylglycine)	6.22 ± 0.38	5.83 ± 0.15	0.024
1,5-Anhydroglucitol (1,5-AG)	6.02 ± 0.33	5.58 ± 0.32	0.049
Nicotinate	4.78 ± 0.34	4.39 ± 0.15	0.018
Ethanolamine	6.88 ± 0.46	6.36 ± 0.24	0.025
myo-Inositol	6.35 ± 0.39	5.81 ± 0.33	0.031
scyllo-inositol	5.14 ± 0.63	4.43 ± 0.24	0.016
Glycylproline	5.43 ± 0.36	4.92 ± 0.15	0.005

[a]For comparison between ART-naive and -experienced patients.
Data represent relative abundance ($\log_{10}$, mean ± SD; $n = 5$).

common opportunistic infections associated with HIV infection (Costa et al., 2006; Patton et al., 2002). In this regard, several studies have shown that tryptophan directly influences *Candida* growth (*in vitro* and *in vivo*) and morphology. The enzyme indole dioxygenase (IDO) converts tryptophan to picolinic acid (PLA), which inhibits the yeast–hyphal transition of *Candida* (Bozza et al., 2005). Blasi et al. (1993) demonstrated that intraperitoneal administration of PLA has a protective effect on mice intracerebrally infected with lethal doses of *C. albicans*. Tryptophan has also been reported to modulate the activity of *Candida* chorismate mutase (a candidal enzyme) and anyhdrase enzymes, which regulates Phe-to-Tyr conversion and carbon utilization, respectively (Bode and Birnbaum, 1991; Bode et al., 1984; Isik et al., 2009). In addition to its direct effect on *Candida*, tryptophan can influence bacteria that are important components of the polymicrobial oral milieu. In this regard, *Candida* converts Trp to β-indolethanol (IEA) and β-indolelactic acid (ILA), both of which inhibit the growth of Gram-positive and Gram-negative bacteria (Narayanan and Rao, 1976). It is possible that the differential levels of metabolites detected in our study may be associated with *Candida* colonization in the mouth of study participants. However, such association could not be investigated because the collected samples were not cultured. Future studies should investigate whether changes in oral metabolites may be associated with *Candida* colonization of the oral cavity.

Several studies have reported that PLA mediates interactions between the host immune cells and fungi by several mechanisms including modulation of the production of reactive oxygen species (Diamond et al., 1980), inhibition of neutrophil-mediated killing of *Candida* pseudohyphae (Wagner et al., 1986), inducing the production of interferon-γ (Mucci et al., 2003), and augmenting the anti-*Candida* activity of neutrophils (Abe et al., 2004). In addition, tryptophan catabolites (a mixture of 3-hydroxykynurenine, 3-hydroxyanthranilic acid, and quinolinic acid) increased expression of Foxp3 mRNA and concomitantly upregulated IL-10 production in *Candida*-pulsed T cells (De Luca et al., 2007). It is possible that changes in oral tryptophan levels and its regulators like IDO and PLA may be associated with T-cell function and apoptosis in HIV-infected patients. Detailed studies are warranted to investigate this potential association.

Tryptophan is converted by microbial aldehyde dehydrogenase to indole-3-acetic acid (IAA), a plant auxin that has also been identified in bacteria (Barash and Manulis-Sasson, 2009; Patten & Glick, 1996) and fungi (Gruen, 1959; Thimann, 1935). Rao et al. (2010) showed that IAA stimulates filamentation in *C. albicans*, thus suggesting a role in *Candida* pathogenesis. However, we found that IAA levels remained similar between the healthy, ART-naive and ART-experienced sample groups ($p \geq 0.234$). This lack of a concomitant increase in IAA levels with tryptophan in the tested samples may be due to the fact that yeast cells have been shown to synthesize IAA using both tryptophan-dependent and -independent pathways (Rao et al., 2010). Further investigation is warranted to explore the association between tryptophan and host immunity as well as the polymicrobial constituents of the oral microbiome.

Among the nucleic acids detected, levels of allantoin, thymine, and AMP were elevated in HIV-infected participants. Allantoin is produced in most mammals by oxidation of uric acid in a conversion catalyzed by the peroxisomal enzyme urate oxidase (or uricase, EC 1.7.3.3), but this enzyme activity is absent in humans (Varela-Echavarria et al., 1988). Detection of allantoin in the oral samples analyzed in the current study suggests the possibly that it is derived from oral microbes. In this regard, allantoin has been identified as a degradation product of microbial metabolism of purines and pyrimideins (Cooper, 1984; Vogels and Van der Drift, 1976). Under nitrogen-deprived conditions, yeast can use allantoin as a nitrogen source and accumulate it in vacuoles as a reserve (Cooper, 1984). Genes involved in nitrogen metabolic regulation (e.g., *GLN3*, a key regulator of allantoin metabolism) have been suggested to cooperate with multiple positive-acting, pathway-

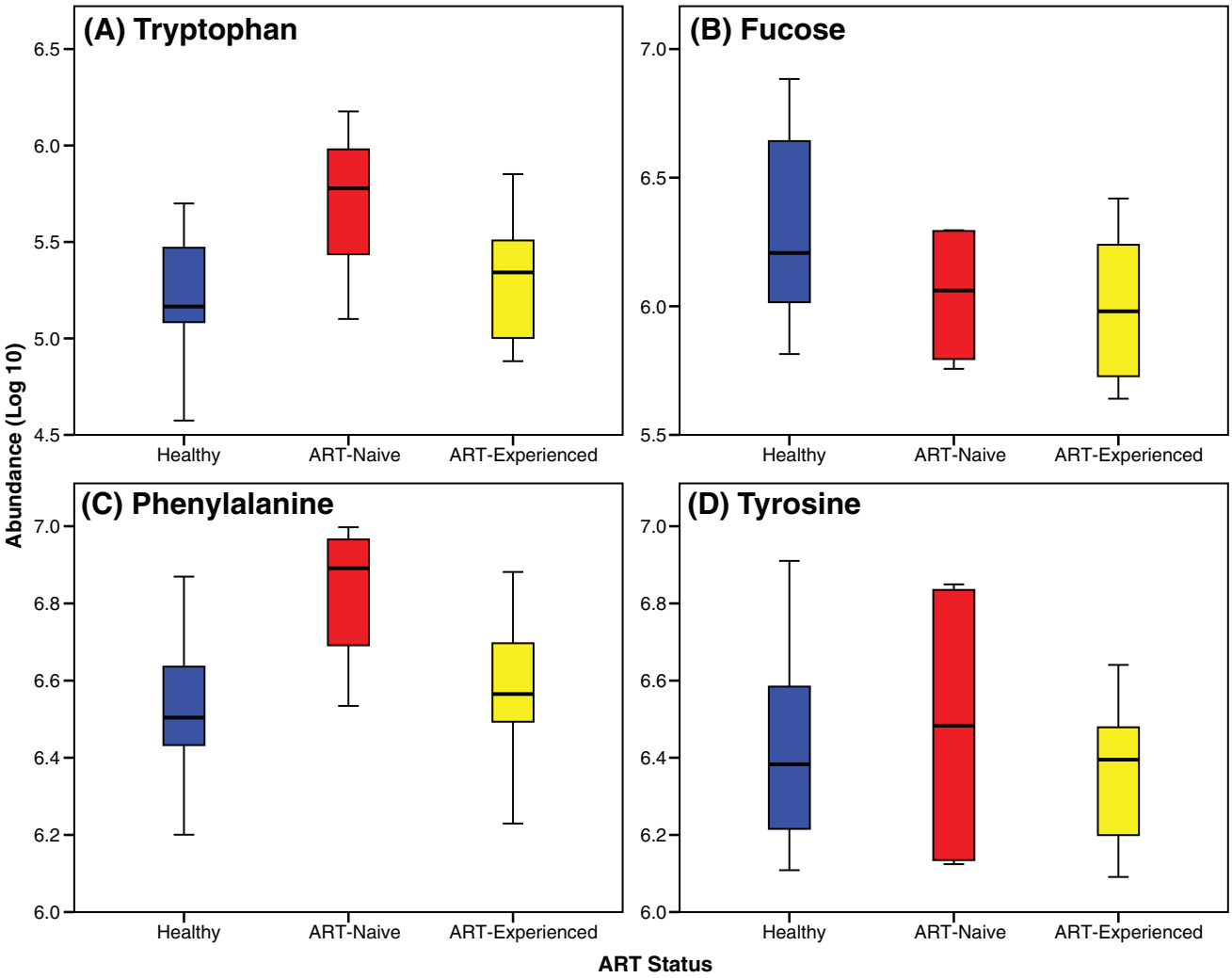

FIG. 3. Levels of representative amino acids and carbohydrates in oral wash samples obtained from healthy and HIV-infected patients. (**A**) Tryptophan; (**B**) fucose; (**C**) Phenylalanine; (**D**) Tyrosine.

specific regulatory proteins to turn on specific sets of nitrogen catabolic genes, and contribute to the pathogenicity of fungal pathogens (Marzluf, 1997).

All carbohydrate compounds that were significantly different between HIV-infected and healthy subjects were lower in samples collected from HIV-infected patients. These included amino sugars, pyruvate, xylose, and fumarate. Although sucrose levels were significantly different between the healthy controls and HIV-infected patients, the mean value in this case was driven strongly by one healthy subject who had extremely high levels of the compound. Therefore, the high level of sucrose is unlikely to have any physiological relevance.

Our results showed that oral wash samples obtained from ART-naive HIV-infected patients exhibited increased oral Phe:Tyr ratio, which was reduced in ART-experienced patients to similar levels as seen in healthy subjects. Interestingly, in a recent study, Zangerle et al. (2010) showed that the Phe:Tyr ratio of serum can be used to monitor immune activation in cancer and HIV-infected patients. Because we used oral wash samples in our study, it is possible that this ratio may have utility in monitoring the immune status (activation) and/or therapy compliance in HIV-infected patients and their response to ART by sampling oral wash, which is noninvasive and presents minimal risks for healthcare workers who manage these patients. It is also possible that changes in metabolite levels may be linked to viral replication because patients on ART had low viral loads. Finally, because the controls in our study were students and staff members from CWRU School of Dental Medicine and School of Medicine, it is possible that they had higher awareness and different practice of dental hygiene than the study group. Controlled clinical trials need to be performed to assess the association of changes in oral metabolite levels with these different variables.

Conclusions

Our metabolomics analysis revealed that oral metabolites are differentially present in HIV-infected patients, relative to healthy controls. These studies represent our attempt to begin addressing the critical gap in knowledge regarding how changes in the oral metabolome correlate with HIV disease. Discovery and identification of novel oral metabolites, and

their interactions will provide insight into the role of oral metabolites in HIV-infected patients and the identification of diagnostic targets.

Acknowledgments

This work was supported by funds from the National Institutes of Health (NIH) BRS ACURE-Q0600136 to the Oral HIV/AIDS Research Alliance (OHARA), NIH/NIAID (RO1 AI035097), and NIH/NIDCR (R01 DE017486-01A1 and R01DE 13932-4), the Bristol Myers Squibb Freedom to Discover Award to M.A.G., NIH/NIAID (1R21AI074077-01A2) to P.K.M., and 1P01-DE019759-01 and 1K23-DE016110-01K to R.J.J. The funders had no role in study design, data collection and analysis, decision to publish, or preparation of the manuscript. The authors wish to acknowledge excellent assistance provided by Metabolon, Inc.

Author Disclosure Statement

The authors declare that no conflicting financial interests exist.

References

Abe, S., Hu, W., Ishibashi, H., Hasumi, K., and Yamaguchi, H. (2004). Augmented inhibition of *Candida albicans* growth by murine neutrophils in the presence of a tryptophan metabolite, picolinic acid. J Infect Chemother 10, 181–184.

Barash, I., and Manulis-Sasson, S. (2009). Recent evolution of bacterial pathogens: the gall-forming *Pantoea agglomerans* case. Annu Rev Phytopathol 47, 133–152.

Barnes, V.M., Teles, R., Trivedi, H.M., Devizio, W., Xu, T., Mitchell, M.W., et al. (2009). Acceleration of purine degradation by periodontal diseases. J Dent Res 88, 851–855.

Blasi, E., Mazzolla, R., Pitzurra, L., Barluzzi, R., and Bistoni, F. (1993). Protective effect of picolinic acid on mice intracerebrally infected with lethal doses of *Candida albicans*. Antimicrob Agents Chemother 37, 2422–2426.

Bode, R., and Birnbaum, D. (1991). Regulation of chorismate mutase activity of various yeast species by aromatic amino acids. Antonie Van Leeuwenhoek 59, 9–13.

Bode, R., Melo, C., and Birnbaum, D. (1984). Absolute dependence of phenylalanine and tyrosine biosynthetic enzyme on tryptophan in *Candida maltosa*. Hoppe Seylers Z Physiol Chem 365, 799–803.

Bozza, S., Fallarino, F., Pitzurra, L., Zelante, T., Montagnoli, C., Bellocchio, S., et al. (2005). A crucial role for tryptophan catabolism at the host/*Candida albicans* interface. J Immunol 174, 2910–2918.

Burchell, B., and Coughtrie, M.W. (1997). Genetic and environmental factors associated with variation of human xenobiotic glucuronidation and sulfation. Environ Health Perspect 105(Suppl 4), 739–747.

Cantor, G.H. (2010). Metabolomics and mechanisms: sometimes the fisher catches a big fish. Toxicol Sci 118, 321–323.

Cline, M.S., Smoot, M., Cerami, E., Kuchinsky, A., Landys, N., Workman, C., et al. (2007). Integration of biological networks and gene expression data using Cytoscape. Nat Protoc 2, 2366–2382.

Cooper, T.G. (1984). Allantoin degradation by *Saccharomyces cerevisiae*—a model system for gene regulation and metabolic integration. Adv Enzymol Relat Areas Mol Biol 56, 91–139.

Costa, C.R., Cohen, A.J., Fernandes, O.F., Miranda, K.C., Passos, X.S., Souza, L.K., et al. (2006). Asymptomatic oral carriage of *Candida* species in HIV-infected patients in the highly active antiretroviral therapy era. Rev Instit Med Trop Sao Paulo 48, 257–261.

Curtius, H.C., Mettler, M., and Ettlinger, L. (1976). Study of the intestinal tyrosine metabolism using stable isotopes and gas chromatography-mass spectrometry. J Chromatogr 126, 569–580.

Dehaven, C.D., Evans, A.M., Dai, H., and Lawton, K.A. (2010). Organization of GC/MS and LC/MS metabolomics data into chemical libraries. J Cheminform 2, 9.

De Luca, A., Montagnoli, C., Zelante, T., Bonifazi, P., Bozza, S., Moretti, S., et al. (2007). Functional yet balanced reactivity to *Candida albicans* requires TRIF, MyD88, and IDO-dependent inhibition of Rorc. J Immunol 179, 5999–6008.

Denkert, C., Budczies, J., Kind, T., Weichert, W., Tablack, P., Sehouli, J., et al. (2006). Mass spectrometry-based metabolic profiling reveals different metabolite patterns in invasive ovarian carcinomas and ovarian borderline tumors. Cancer Res 66, 10795–10804.

Denkert, C., Budczies, J., Weichert, W., Wohlgemuth, G., Scholz, M., Kind, T., et al. (2008). Metabolite profiling of human colon carcinoma—deregulation of TCA cycle and amino acid turnover. Mol Cancer 7, 72.

Diamond, R.D., Clark, R.A., and Haudenschild, C.C. (1980). Damage to *Candida albicans* hyphae and pseudohyphae by the myeloperoxidase system and oxidative products of neutrophil metabolism in vitro. J Clin Invest 66, 908–917.

Diehl, S.R. (2006). Pulling teeth into the genomics era. J Am Dent Assoc 137, 710, 712, 714.

Evans, A.M., Dehaven, C.D., Barrett, T., Mitchell, M., and Milgram, E. (2009). Integrated, nontargeted ultrahigh performance liquid chromatography/electrospray ionization tandem mass spectrometry platform for the identification and relative quantification of the small-molecule complement of biological systems. Anal Chem 81, 6656–6667.

Gao, J., Tarcea, V.G., Karnovsky, A., Mirel, B.R., Weymouth, T.E., Beecher, C.W., et al. (2010). Metscape: a Cytoscape plug-in for visualizing and interpreting metabolomic data in the context of human metabolic networks. Bioinformatics 26, 971–973.

Garcia, I., and Tabak, L.A. (2008). Beyond the "omics": translating science into improved health. J Am Dent Assoc 139, 392–395.

Giacomelli, L., and Covani, U. (2010). Bioinformatics and data mining studies in oral genomics and proteomics: new trends and challenges. Open Dent J 4, 67–71.

Gruen, H.E. (1959). On the plant growth hormone produced by *Rhizopus suinus*. Annu Rev Plant Physiol 10, 405–440.

Isik, S., Kockar, F., Aydin, M., Arslan, O., Guler, O.O., Innocenti, A., et al. (2009). Carbonic anhydrase activators: activation of the beta-carbonic anhydrase Nce103 from the yeast *Saccharomyces cerevisiae* with amines and amino acids. Bioorg Med Chem Lett 19, 1662–1665.

Katz, I.J., Gerntholtz, T.E., Van Deventer, M., Schneider, H., and Naicker, S. (2010). Is there a need for early detection programs for chronic kidney disease? Clin Nephrol 74, 113–118.

Levine, M., Progulske-Fox, A., Denslow, N.D., Farmerie, W.G., Smith, D.M., Swearingen, W.T., et al. (2001). Identification of lysine decarboxylase as a mammalian cell growth inhibitor in *Eikenella corrodens*: possible role in periodontal disease. Microb Pathog 30, 179–192.

Marzluf, G.A. (1997). Genetic regulation of nitrogen metabolism in the fungi. Microbiol Mol Biol Rev 61, 17–32.

Morgenthal, K., Weckwerth, W., and Steuer, R. (2006). Metabolomic networks in plants: transitions from pattern recognition to biological interpretation. Biosystems 83, 108–117.

Mucci, A., Varesio, L., Neglia, R., Colombari, B., Pastorino, S., and Blasi, E. (2003). Antifungal activity of macrophages engineered to produce IFNgamma: inducibility by picolinic acid. Med Microbiol Immunol 192, 71–78.

Naicker, S., and Fabian, J. (2010). Risk factors for the development of chronic kidney disease with HIV/AIDS. Clin Nephrol 74, 51–56.

Narayanan, T.K., and Rao, G.R. (1976). Beta-indoleethanol and beta-indolelactic acid production by Candida species: their antibacterial and autoantibiotic action. Antimicrob Agents Chemother 9, 375–380.

Ohta, T., Masutomi, N., Tsutsui, N., Sakairi, T., Mitchell, M., Milburn, M.V., et al. (2009). Untargeted metabolomic profiling as an evaluative tool of fenofibrate-induced toxicology in Fischer 344 male rats. Toxicol Pathol 37, 521–535.

Patten, C.L., and Glick, B.R. (1996). Bacterial biosynthesis of indole-3-acetic acid. Can J Microbiol 42, 207–220.

Patton, L.L., Phelan, J.A., Ramos-Gomez, F.J., Nittayananta, W., Shiboski, C.H., and Mbuguye, T.L. (2002). Prevalence and classification of HIV-associated oral lesions. Oral Dis 8(Suppl 2), 98–109.

Pendyala, G., Want, E.J., Webb, W., Siuzdak, G., and Fox, H.S. (2007). Biomarkers for neuroAIDS: the widening scope of metabolomics. J Neuroimmune Pharmacol 2, 72–80.

Rao, R.P., Hunter, A., Kashpur, O., and Normanly, J. (2010). Aberrant synthesis of indole-3-acetic acid in *Saccharomyces cerevisiae* triggers morphogenic transition, a virulence trait of pathogenic fungi. Genetics 185, 211–220.

Rosenberg, M. (2002). The science of bad breath. Sci Am 286, 72–79.

Schepers, E., Meert, N., Glorieux, G., Goeman, J., Van der Eycken, J., and Vanholder, R. (2007). P-cresylsulphate, the main in vivo metabolite of *p*-cresol, activates leucocyte free radical production. Nephrol Dial Transplant 22, 592–596.

Scully, C., El-Maaytah, M., Porter, S.R., and Greenman, J. (1997). Breath odor: etiopathogenesis, assessment and management. Eur J Oral Sci 105, 287–293.

Sedgley, C.M., and Samaranayake, L.P. (1994). The oral prevalence of aerobic and facultatively anaerobic Gram-negative rods and yeasts in Hong Kong Chinese. Arch Oral Biol 39, 459–466.

Shah, P., Nanduri, B., Swiatlo, E., Ma, Y., and Pendarvis, K. (2010). Polyamine biosynthesis and transport mechanisms are crucial for fitness and pathogenesis of *Streptococcus pneumoniae*. Microbiology Oct 21 [Epub Ahead of Print].

Shannon, P., Markiel, A., Ozier, O., Baliga, N.S., Wang, J.T., Ramage, D., et al. (2003). Cytoscape: a software environment for integrated models of biomolecular interaction networks. Genome Res 13, 2498–2504.

Shiboski, C.H., Patton, L.L., Webster-Cyriaque, J.Y., Greenspan, D., Traboulsi, R.S., Ghannoum, M., et al. (2009). The Oral HIV/AIDS Research Alliance: updated case definitions of oral disease endpoints. J Oral Pathol Med 38, 481–488.

Sreekumar, A., Poisson, L.M., Rajendiran, T.M., Khan, A.P., Cao, Q., Yu, J., et al. (2009). Metabolomic profiles delineate potential role for sarcosine in prostate cancer progression. Nature 457, 910–914.

Sugimoto, M., Wong, D.T., Hirayama, A., Soga, T., and Tomita, M. (2010). Capillary electrophoresis mass spectrometry-based saliva metabolomics identified oral, breast and pancreatic cancer-specific profiles. Metabolomics 6, 78–95.

Suzzi, G., and Gardini, F. (2003). Biogenic amines in dry fermented sausages: a review. Int J Food Microbiol 88, 41–54.

Takei, M., Ando, Y., Saitoh, W., Tanimoto, T., Kiyosawa, N., Manabe, S., et al. (2010). Ethylene glycol monomethyl ether-induced toxicity is mediated through the inhibition of flavoprotein dehydrogenase enzyme family. Toxicol Sci 118, 643–652.

Thimann, K.V. (1935). On the plant growth hormone produced by *Rhizopus suinus*. J Biol Chem 109, 279–291.

Varela-Echavarria, A., Montes de Oca-Luna, R., and Barrera-Saldana, H.A. (1988). Uricase protein sequences: conserved during vertebrate evolution but absent in humans. FASEB J 2, 3092–3096.

Vogels, G.D., and Van der Drift, C. (1976). Degradation of purines and pyrimidines by microorganisms. Bacteriol Rev 40, 403–468.

Volberding, P.A., and Deeks, S.G. (2010). Antiretroviral therapy and management of HIV infection. Lancet 376, 49–62.

Wagner, D.K., Collins-Lech, C., and Sohnle, P.G. (1986). Inhibition of neutrophil killing of *Candida albicans* pseudohyphae by substances which quench hypochlorous acid and chloramines. Infect Immun 51, 731–735.

Walters, J.D. (1987). Polyamine analysis of human gingival crevicular fluid. J Periodontal Res 22, 522–523.

White, P.L., Williams, D.W., Kuriyama, T., Samad, S.A., Lewis, M.A.O., and Barnes, R.A. (2004). Detection of *Candida* in concentrated oral rinse cultures by real-time PCR. J Clin Microbiol 42, 2101–2107.

Yan, S.K., Wei, B.J., Lin, Z.Y., Yang, Y., Zhou, Z.T., and Zhang, W.D. (2008). A metabonomic approach to the diagnosis of oral squamous cell carcinoma, oral lichen planus and oral leukoplakia. Oral Oncol 44, 477–483.

Zangerle, R., Kurz, K., Neurauter, G., Kitchen, M., Sarcletti, M., and Fuchs, D. (2010). Increased blood phenylalanine to tyrosine ratio in HIV-1 infection and correction following effective antiretroviral therapy. Brain Behav Immun 24, 403–408.

Zhou, J., Xu, B., Huang, J., Jia, X., Xue, J., Shi, X., et al. (2009). 1H NMR-based metabonomic and pattern recognition analysis for detection of oral squamous cell carcinoma. Clin Chim Acta 401, 8–13.

Address correspondence to:
Mahmoud Ghannoum, PhD
Center for Medical Mycology
Department of Dermatology
Case Western Reserve University
11100 Euclid Avenue
Cleveland, OH 44106-5028

E-mail: Mahmoud.Ghannoum@case.edu